Scintillation properties of $Lu_2Si_2O_7:Ce^{3+}$, a fast and efficient scintillator crystal

2003 J. Phys.: Condens. Matter 15 2091

(http://iopscience.iop.org/0953-8984/15/12/326)

INSTITUTE OF PHYSICS PUBLISHING JOURNAL OF PHYSICS: CONDENSED MATTER

J. Phys.: Condens. Matter **15** (2003) 2091–2102 PII: S0953-8984(03)58989-5

Scintillation properties of $Lu_2Si_2O_7:Ce^{3+}$, a fast and efficient scintillator crystal

L Pidol[1,2], A Kahn-Harari[1], B Viana[1], B Ferrand[3], P Dorenbos[4], J T M de Haas[4], C W E van Eijk[4] and E Virey[2]

[1] Ecole Nationale Supérieure de Chimie de Paris (ENSCP), Laboratoire de Chimie Appliquée de l'Etat Solide, UMR-CNRS 7574, 11 rue Pierre et Marie Curie, 75231 Paris Cedex 05, France
[2] Saint Gobain Cristaux et Détecteurs, 104 route de Larchant, 77140 Saint Pierre les Nemours, France
[3] LETI/DOPT/STCO/Laboratoire Cristallogenèse Appliquée—CEA Grenoble, 17 rue des Martyrs, 38054 Grenoble Cedex 09, France
[4] Interfaculty Reactor Institute, Delft University of Technology, Mekelweg 15, 2629 JB Delft, The Netherlands

E-mail: viana@ext.jussieu.fr

Received 31 January 2003
Published 17 March 2003
Online at stacks.iop.org/JPhysCM/15/2091

Abstract

Cerium doped lutetium pyrosilicate $Lu_2Si_2O_7:Ce^{3+}$ (LPS), a new inorganic scintillator, displays particularly promising performance. This material can be readily pulled from the melt. A high light output (average value: 26 300 ph MeV^{-1}), a relatively good energy resolution (9%) and a fast decay time (38 ns) without afterglow make this new scintillator very attractive, in particular for medical imaging. Optical characterizations and scintillation properties of LPS:Ce large single crystals are presented, including timing properties and study of the scintillation yields as a function of incident energy.

1. Introduction

Scintillator crystals are used to detect gamma rays or x-rays in many applications like computerized tomography (CT), positron emission tomography (PET), nuclear and particle physics experiments or geophysical exploration. A scintillator crystal converts a fraction of the energy deposited by the incident gamma ray or x-ray into a burst of visible or ultraviolet photons which is then converted into an electrical signal by a photomultiplier tube (PMT) or a photodiode optically coupled to the crystal. The ideal scintillator should have high density and high effective atomic number for a high stopping power of gamma rays, a high scintillation light yield (LY) for measuring the gamma ray energy accurately and a short decay time for high count-rate capability [1]. A number of cerium doped oxide based scintillators have recently been developed, like GSO (Gd_2SiO_5:Ce) [2], LSO (Lu_2SiO_5:Ce) [3], LuAP ($LuAlO_3$:Ce) [4, 5] and LYSO ($Lu_{2(1-x)}Y_{2x}SiO_5$:Ce) [6, 7]. These materials tend to exhibit the desired qualities

Table 1. Physical and scintillation properties of several scintillators.

	BGO $Bi_4Ge_3O_{12}$	GSO:Ce Gd_2SiO_5	LSO:Ce Lu_2SiO_5	LuAP:Ce $LuAlO_3$	LPS:Ce $Lu_2Si_2O_7$
Melting point (°C)	1050	1950	2100	1960	1900
Density (g cm^{-3})	7.13	6.7	7.4	8.34	6.23
Effective atomic number	75	59	66	65	64
Attenuation length for a 511 keV photon (cm)	1.12	1.38	1.14	1.05	1.38
Refractive index	2.15	1.89	1.81	1.94	1.74
LY (photons MeV^{-1})	8200	8500	25 000	11 300	26 300
Emission wavelength (nm)	480	430	420	365	385
Decay times	300 ns	56 ns, 600 ns	40 ns, >2000 s	18 ns	38 ns
Time resolution (ps)	1000	700	160	160	253

for gamma detection scintillators: a high density, a scintillation decay time shorter than 100 ns and a light output exceeding that of BGO ($Bi_4Ge_3O_{12}$), which is still commonly used for gamma detection.

In this paper, we have characterized the scintillation properties of cerium doped lutetium pyrosilicate, $Lu_2Si_2O_7$ (LPS:Ce), a new material which is suitable for applications such as PET or oil well logging. Following the first successful studies with LPS:Ce crystals prepared by the floating zone melting technique [1, 8], optically clear Czochralski grown LPS boules were grown with desired properties for gamma-ray detection [9]. The main properties are gathered in table 1, together with properties of some other already studied scintillators.

2. Experimental details

LPS crystals were grown from the melt (1900 °C) by a vertical pulling method (Czochralski process) using an iridium crucible. A LPS crystal was used as a seed. Both undoped LPS ($Lu_2Si_2O_7$) and Ce doped LPS ($Lu_{2(1-x)}Ce_{2x}Si_2O_7$) were grown, with a cerium concentration in the melt ranging from 0.25 to 0.5%. Samples of about 1 cm^3 were cut and polished for scintillation measurements (table 2).

Optical absorption experiments were done using a CARY 5 Varian spectrophotometer. Emission measurements and decay time profiles under UV excitation were performed with the excitation wavelength coming from the third harmonic of a YAG:Nd laser ($\lambda_{exc} = 355$ nm). The light was analysed with a UV enhanced ICCD (Princeton) detector. Optical spectra were recorded at temperatures ranging from 10 to 300 K with a CTI-Cryogenics refrigeration system. Between 300 and 600 K, we used a home-made heating device. The temperature accuracy was ± 2 K.

X-ray excited optical luminescence spectra were recorded using an x-ray tube with a Cu anode, operating at 35 kV and 25 mA, at temperatures ranging from 200 to 400 K. The emission was dispersed with an ARC VM504 monochromator (blazed at 300 nm, 1200 grooves mm^{-1}) and measured with an EMI 9462 PMT. The data were corrected for the wavelength dependence of the PMT quantum efficiency and for the monochromator response.

Scintillation decay time spectra, under ^{137}Cs 662 keV γ-ray excitation, were recorded with two Philips XP2020Q PMTs using standard start–stop techniques as described in [10].

To evaluate the possible afterglow, crystals were first heated for several minutes at 672 K and then exposed to x-ray irradiation for 50 s (Cu anode, 35 kV and 25 mA). Next, a Hamamatsu R943-02 PMT was used to measure the emission intensity for several hours after this exposure and results were normalized per milligram of material.

The thermoluminescence (TL) glow curves were recorded with a linear heating rate from 313 to 672 K. Prior to each TL experiment, the crystals (0.5 mm thick) were annealed for several minutes at 672 K. Next, they were exposed for 20 s to β-irradiation ($^{90}Sr/^{90}Y$ source providing a dose of 1 mGy s^{-1} in air). TL glow curves were recorded in N_2 atmosphere with a 0.5 K s^{-1} heating rate, using a TL/OSL system (TL-DA-15) from Risø.

To determine the absolute and relative light yields (LY), the crystal under investigation was mounted using an optical coupling compound (Viscasil 60 000 cSt General Electric) to the window of a Hamamatsu R1791 PMT. Crystals were covered with several layers of 0.1 mm thick ultraviolet reflecting Teflon tape. The absolute photoelectron LY was obtained by comparing the 662 keV photopeak position in the pulse height spectrum of a ^{137}Cs source with the maximum position in the pulse height spectrum of single photoelectron from the photocathode. More details about the pulse height experiments are given elsewhere [11]. For excitation energies varying between 60 keV and 1.22 MeV, ^{241}Am, ^{137}Cs and ^{22}Na γ-ray sources were used. An Amersham (code AMC.2084) variable x-ray source was used to excite the crystals at energies ranging between 13.5 and 44.5 keV. In this source, ^{241}Am produces characteristic Kα and Kβ x-rays from Rb, Mo, Ag, Ba and Tb targets. The relative LYs were then obtained by comparing the absolute LY for different energies, with the absolute LY under ^{137}Cs-excitation (662 keV).

The coincidence timing experiment was carried out with two LPS:0.5% Ce crystals ($4 \times 1 \times 20$ mm^3) coupled to XP2020Q PMTs. The measurements were performed for a ^{60}Co source and constant-fraction timing with an energy threshold set at $E \geqslant 1$ MeV.

3. Results and discussion

3.1. Crystal structure

$Lu_2Si_2O_7$ presents the thorveitite structure, with monoclinic symmetry, space group $C2/m$. It has a single crystallographic site for lutetium ions, with six oxygen neighbours. It is a distorted octahedral site, with C_2 symmetry. The lattice constants were refined to values $a = 6.765$ Å, $b = 8.838$ Å, $c = 4.715$ Å, $\beta = 101.98°$ and $V = 275.1$ $Å^3$. These values are similar to the unit cell constants already reported for undoped LPS [12], since the cerium concentration is too low to affect the lattice constants.

3.2. Optical properties

In figure 1(a), the absorption spectrum of $Lu_2Si_2O_7$ doped with 0.5% Ce (in the melt), at room temperature, is presented. The Ce doped crystals display two absorption bands centred at 303 and 349 nm, corresponding to transitions from the 4f ground state to the 5d sublevels of Ce^{3+}. As cerium ions replace lutetium in a low symmetry site, it is likely that the 5d levels are split by the crystal field interaction into more than two components. These bands cannot be seen under these experimental conditions.

Figure 1(b) shows the Ce^{3+} emission, at room temperature, under 355 nm excitation. It consists of a broad and structured band with a maximum at 378 nm and a shoulder around 405 nm. At low temperature, the two peaks are sharper on the emission spectrum and resolved into two bands at 376 and 405 nm respectively. These peaks are attributed to transitions from the Ce^{3+}-5d lowest energy level to the $^2F_{7/2}$ and $^2F_{5/2}$ manifolds split by the spin–orbit interaction. The splitting energy value between the $^2F_{7/2}$ and $^2F_{5/2}$ levels is 1904 cm^{-1}. The Stokes shift for the Ce^{3+} doped LPS is about 2200 cm^{-1} at room temperature, a typical value for this luminescent ion [13].

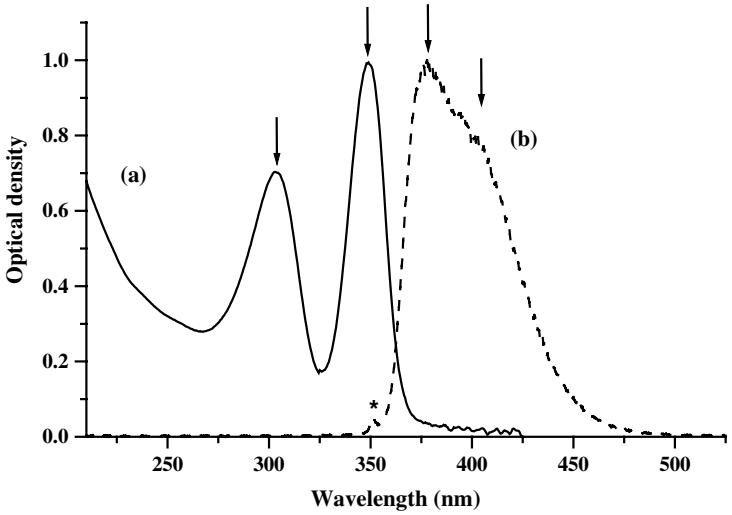

Figure 1. Optical characteristics of the $Lu_2Si_2O_7$:0.5% Ce crystal (1 mm thick) at room temperature: (a) absorption spectrum; (b) emission spectrum under a 355 nm excitation wavelength. Bands are indicated by arrows. The small peak marked by a star is an artifact due to the laser excitation.

Compared to UV excitation, x-ray induced emission at room temperature, gives a very similar result (figure 2). Whatever the excitation, only one type of Ce^{3+} emission is observed. It is linked to the fact that the lutetium pyrosilicate structure offers a single site for Ce^{3+}.

Under x-ray excitation, we have measured the emission intensity as function of temperature for LPS:0.5% Ce. The luminescence efficiency remains very high when the temperature increases. It even increases when the temperature varies between 200 and 400 K as presented in figure 3. This could allow the LPS:Ce scintillation detectors to be used under relatively high temperature conditions.

3.3. Decay time under UV and gamma irradiation

Figure 4 shows the decay time spectra of LPS:Ce under UV excitation ($\lambda_{exc} = 355$ nm) and gamma ray excitation (^{137}Cs source, 662 keV). The solid curves fit the data with a single exponential. The deduced decay times are similar, 37 and 38 ns respectively, under UV and gamma excitation. When LPS:Ce crystals are excited by UV radiation, the Ce^{3+} luminescent centres are directly excited and then the experimental lifetimes are very short, due to the allowed $5d^14f^0 \rightarrow 5d^04f^1$ transition. When LPS crystals are excited with higher energy photons such as gamma rays or x-rays, the scintillation process in LPS:Ce can be divided into two parts:

(1) the creation of electron–hole pairs and the energy transfer to the luminescent Ce^{3+} centres and
(2) the radiative emission of the excited luminescent centres.

Since the observed decay constant under gamma-ray excitation is close to that obtained under UV excitation, the energy transfer to the luminescent centres should be faster than 1 ns, at room temperature.

Figure 5 presents the temperature dependence of the decay time under UV excitation. The rollover point of the decay time is close to 440 K. Two distinct trends are observed.

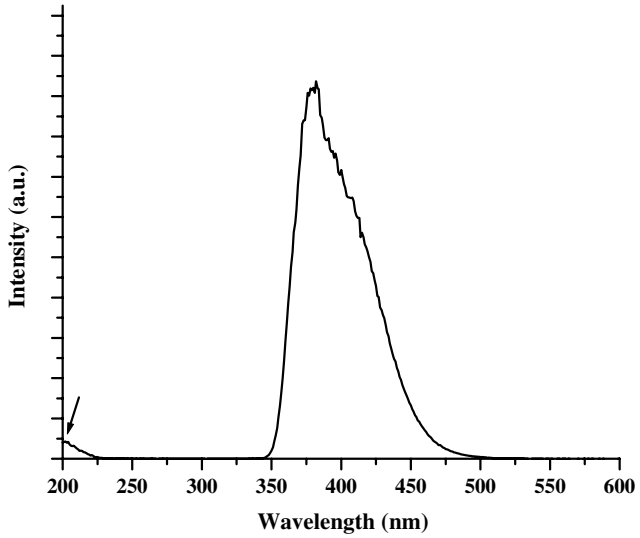

Figure 2. X-ray induced emission spectra for $Lu_2Si_2O_7$:0.5% Ce crystals at room temperature (1 mm thick). The signal near 200 nm, marked with an arrow, is an experimental artifact.

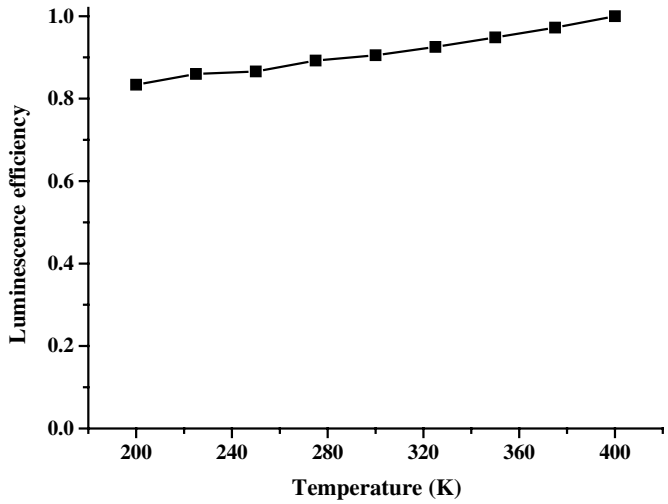

Figure 3. Luminescence efficiency under x-ray excitation of Ce^{3+} in LPS:0.5% Ce (1 mm thick) as a function of temperature. For each temperature, the emission intensity, determined as the total area under the spectral curve of emission, was normalized to the intensity at 400 K. The curve is a guide to the eye.

First, below 440 K, the decay time slightly increases with temperature. Second, beyond 440 K, when the temperature increases, the experimental lifetime strongly decreases. Such temperature dependence of the measured fluorescence lifetimes has already been reported for cerium doped:$YAlO_3$, $Y_3Al_5O_{12}$, CaF_2 and $YLiF_4$ compounds [14]. The total decay rate is given by

$$\tau_{exp}^{-1} = \tau_R^{-1} + \tau_{NR}^{-1} \tag{1}$$

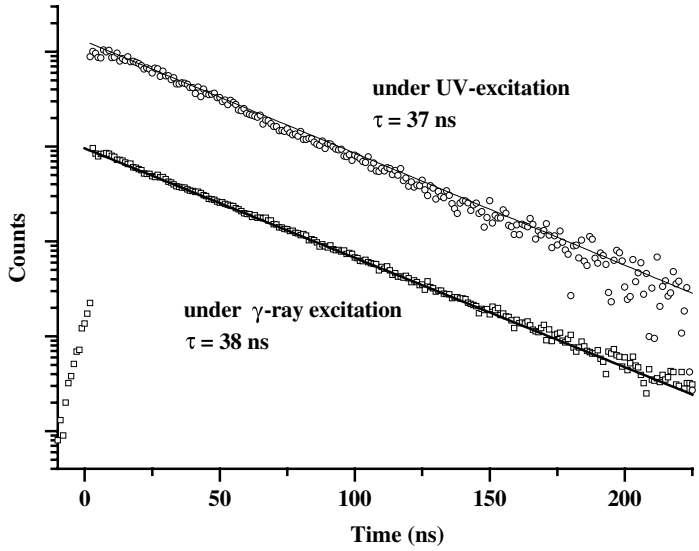

Figure 4. Decay curves of Ce^{3+} in LPS:0.25% Ce crystal ($3.9 \times 8.2 \times 30$ mm^3) at room temperature under UV excitation, $\lambda_{exc} = 355$ nm and $\lambda_{em} = 385$ nm (○), and gamma excitation, with a ^{137}Cs source (□). The solid curves fit the data with a single exponential.

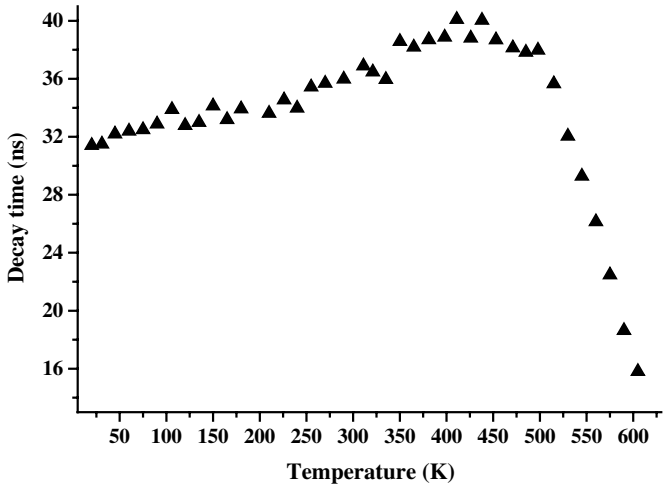

Figure 5. Decay times ($\lambda_{exc} = 355$ nm and $\lambda_{em} = 385$ nm) of Ce^{3+} in LPS:0.5% Ce (1 mm thick) as function of temperature.

where τ_{exp} is the experimental fluorescence lifetime of the 5d–4f transition and τ_R and τ_{NR} are the contributions from radiative and non-radiative processes, respectively. At low temperatures, radiative transitions dominate and a slow linear increase of τ_R could be explained by a photon trapping effect. At higher temperatures, the rapid decrease of the decay time values means that non-radiative de-excitation predominates and should be correlated to a strong quenching of the luminescence efficiency. To confirm that, a study of luminescence efficiency for temperature over 400 K is still necessary. The non-radiative decay rate W_{NR} $(=\tau_{NR}^{-1})$ is calculated from equation (1) for temperatures higher than 440 K. Figure 6 illustrates the temperature variation

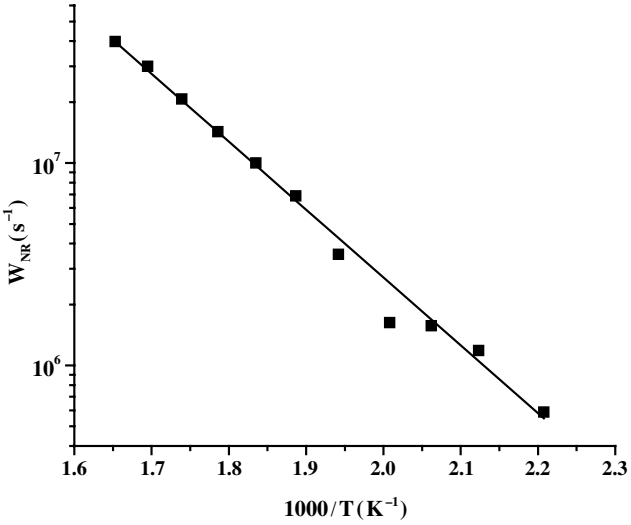

Figure 6. Non-radiative decay rate for Ce^{3+}:LPS as a function of inverse temperature. The solid line fits the data with the Arrhenius equation, $\Delta E = 0.66 \pm 0.01$ eV and $\tau_t = 80 \pm 20$ fs. The non-radiative probability is obtained by subtraction of the radiative contribution linearly extrapolated for temperature above 440 K.

of the deduced non-radiative relaxation rate. The fit was done assuming that W_{NR} varies with temperature, following an Arrhenius law:

$$W_{NR} = \tau_t^{-1} \exp\left(-\frac{\Delta E}{k_B T}\right) \tag{2}$$

where k_B is the Boltzmann constant, the activation energy ΔE is 0.66 ± 0.1 eV and $\tau_t = 80 \pm 20$ ps corresponds to the thermal decay. If we assume, as in [14], that quenching of Ce^{3+} luminescence is caused by autoionization of the 5d electron to the conduction band, then $\Delta E \sim 5400$ cm^{-1} should be related to the energy bandgap between the bottom of the conduction band and the position of the lowest 5d level.

3.4. Afterglow and thermoluminescence

A key parameter for scintillation applications is the afterglow phenomenon. Comparison between afterglow in LSO:Ce and LPS:Ce behaviour is presented in figure 7, using long time recorded luminescence. A previous study on the here-employed LSO sample is described in [15] and [16]. Whereas LSO:Ce presents an exponentially decaying afterglow [15, 17], the LPS:Ce crystal does not show any afterglow in that time range, as observed in figure 7. Actually, for LSO:Ce, after 200 s, the residual intensity induced by the x-ray exposure is about 0.2% of the initial intensity and this intensity is still decreasing after several minutes, pointing out the strong afterglow, well known in the lutetium oxyorthosilicate material. In the case of LPS:Ce, this residual intensity is less than 0.01% after 200 s. Then, it remains at this constant rate, due only to the background intrinsic intensity of ^{176}Lu isotopes in the compound.

TL experiments confirm these observations. Figure 8 shows the thermoluminesence glow curves for LPS:0.25% Ce and LSO:0.2% Ce crystals. This latter sample (LSO6-4) has already been studied in [15] and [16]. After exposure to β-irradiation for 20 s, several peaks are observed when the temperature increases. Our attention is focused on the peak observed just

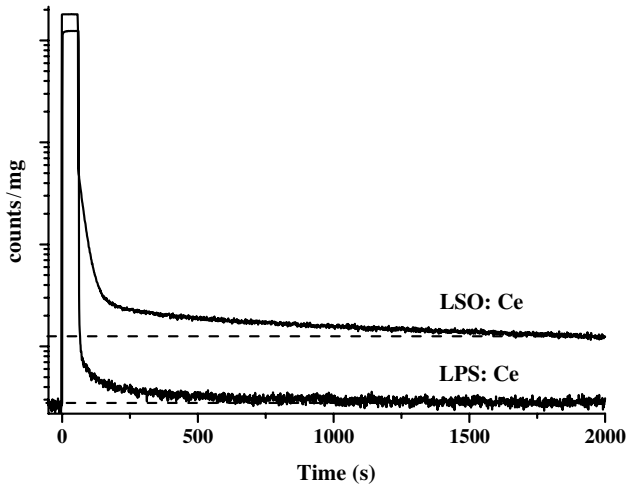

Figure 7. Afterglow luminescence of LPS:0.25% Ce and LSO:0.2% Ce at room temperature. The crystals were exposed for 50 s to an x-ray beam (λ_{Cu}, 35 kV and 25 mA). (The LSO sample is named LSO7-11 in references [15, 16].)

Table 2. LYs and energy resolutions of several $Lu_2Si_2O_7$:Ce crystals under γ-ray excitation (^{137}Cs source 662 keV). Shaping time, 10 μs; LY estimated standard deviation, 10%. Dimensions of the six-sided polished samples are mentioned; cerium concentration corresponds to the initial melt.

Samples	Cerium rate in the melt	Dimensions (mm^3)	LY (ph MeV^{-1})	Energy resolution (%)
1	LPS:0.5% Ce	$3.9 \times 8.2 \times 26.4$	23 310	11.4
2	LPS:0.5% Ce	$9.5 \times 9 \times 10$	25 700	9.5
3	LPS:0.25% Ce	$3.9 \times 8.3 \times 20.5$	28 960	11.9
4	LPS:0.25% Ce	$3.9 \times 8.2 \times 30$	24 800	10.8
5	LPS:0.5% Ce	$5 \times 1.95 \times 31.1$	28 720	10.1

above room temperature (337 and 346 K for LPS and LSO, respectively), which is closely linked to the afterglow phenomenon. For the LPS:Ce crystal, the very low intensity of this peak is in good agreement with the absence of afterglow. In contrast, for the LSO crystal, this peak is very intense, confirming the observed strong afterglow (figure 7). Some authors [18] report that the position of this glow peak depends on the crystallographic structure of oxyorthosilicates. For Gd_2SiO_5, with $P2_1/c$ crystal symmetry, the maximum in the TL curve is observed 50 K higher than for Lu_2SiO_5, with $C2/c$ crystal symmetry. The authors suggest that the crystal structure of these silicates plays an important role in trap creation, which is probably associated with the host metal–ion–ligand configuration. So, major differences between the crystallographic structures, $C2/c$—two sites for the rare-earth ion in LSO—and $C2/m$—one site for the rare earth in LPS, could explain the different behaviours in terms of trap creation and therefore in the afterglow phenomenon.

3.5. Light yields, energy resolution and non-proportionality

Table 2 compiles the LY values and the energy resolution of several LPS:Ce crystals. The average LY is about 26 300 ph MeV^{-1}, with a dispersion about $\pm$3000 ph MeV^{-1}. LPS:Ce

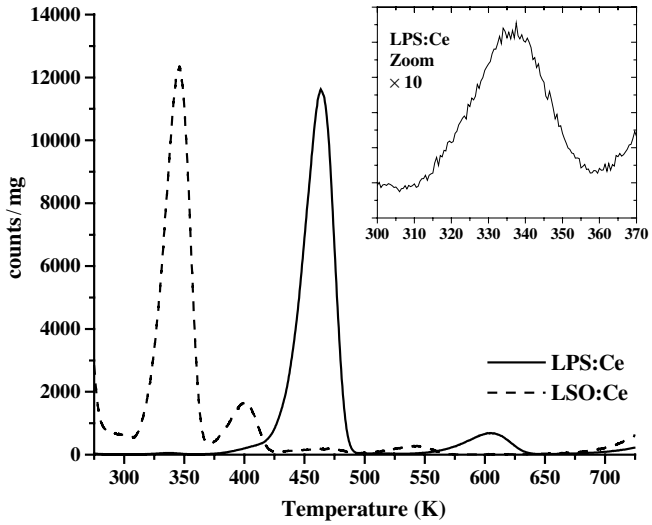

Figure 8. TL glow curves of LPS:0.25% Ce and LSO:0.2% Ce crystals (0.5 mm thick), recorded at a heating rate $\beta = 0.5$ K s^{-1}, after exposure for 20 s to β-irradiation (^{90}Sr/^{90}Y source, 1 mGy s^{-1}). In the inset, the first peak is scaled by a factor of ten for LPS.

crystals present one of the best LYs obtained with a cerium doped oxide based scintillator. The theoretical maximum LY, in photons MeV^{-1}, can be described by the following equation [19]:

$$LY = \frac{10^6 SQ}{\beta E_{gap}} \tag{3}$$

where E_{gap} is the energy gap between valence and conduction bands (about 6.95 eV for LPS), βE_{gap} indicates the average energy required to produce one thermalized electron–hole pair (E_{e-h}), $\beta \approx 2$–3. S is the energy transfer efficiency to the luminescent centre (Ce^{3+}) and Q is the corresponding quantum efficiency, i.e. the efficiency for photon emission once the luminescent centre is excited. By using $S = 1$ and $Q = 1$, the theoretical maximum LY would be about 57 000 ph MeV^{-1} (for $\beta = 2.5$). The difference between theoretical and experimental light outputs could then be linked either to defects present in the material, that could trap electrons or holes created during the process, or to a direct electron–hole recombination process. Several peaks observed around 470 and 600 K in the TL curve (figure 8) confirm the existence of traps in the material. The energy resolution at 662 keV, given by the full width at half maximum (FWHM) of the photopeak, is in the range 9–12%.

Figure 9 shows the pulse height spectrum of an LPS:0.5% Ce crystal excited by a ^{137}Cs source. Also shown in the same picture is the intrinsic background activity from the crystal itself. This background, measured without excitation, arises from the beta decay of the ^{176}Lu isotope, which represents 2.6% of natural Lu abundance. The intrinsic background activity of LPS:Ce is 219 counts s^{-1} cm^{-3}, which is somewhat less than for LSO:Ce or LuAP:Ce (318 and 323 counts s^{-1} cm^{-3} respectively [20]).

To go further into the analysis, the variation of the scintillation response as a function of the incident energy was investigated. Figure 10 shows non-proportional scintillation response curves of three different LPS:Ce polished crystals. For each sample, the light output is approximately divided by two when incident energy decreases from 1 MeV to 14 keV. One can notice a discontinuity around 60 keV where the slope decreases: it could correspond to the K absorption edge at 63.3 keV of lutetium ions. It appears so far that all silicate materials,

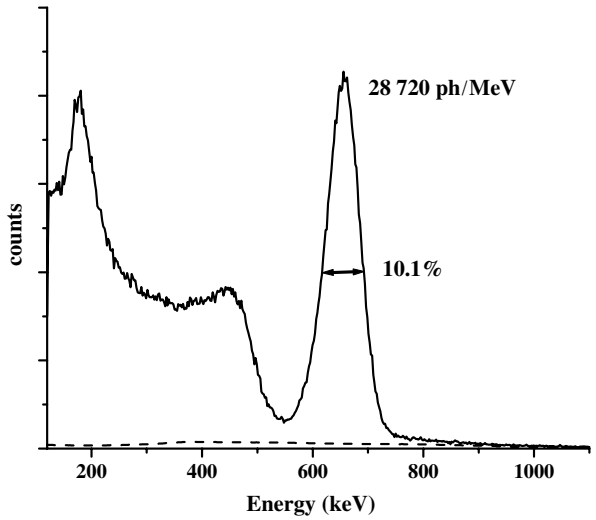

Figure 9. Pulse height spectrum recorded with LPS:0.5% Ce (sample 5) under γ-ray excitation, ^{137}Cs source of 662 keV (solid curve). Pulse height spectrum corresponding to the background, recorded with LPS:0.5% Ce without radioactive source (dashed curve). Shaping time: 10 μs, LY estimated standard deviation: 10%.

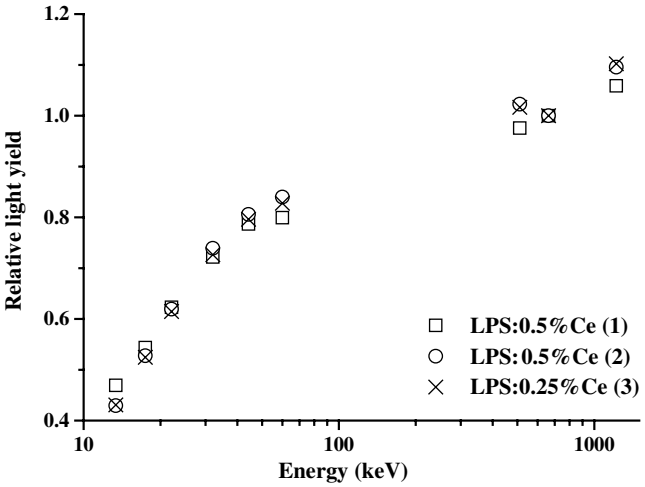

Figure 10. Scintillation LYs for different LPS:Ce crystals, at room temperature, as a function of excitation energy, normalized to the LY at 662 keV excitation. The numbers in brackets refer to the samples of table 2. Shaping time, 3 μs; LY estimated standard deviation, 10%.

like LSO, YSO, GSO or LGSO [21–23], exhibit large non-proportionality in the light output. This suggests that the non-proportionality in the scintillation response could be characteristic of silicate scintillators.

The non-proportional response of the scintillator influences the ultimate energy resolution. The fundamental limit to the energy resolution is primarily determined by the Poisson statistics in the number of photons detected by the PMT. The fundamental limit for energy resolution

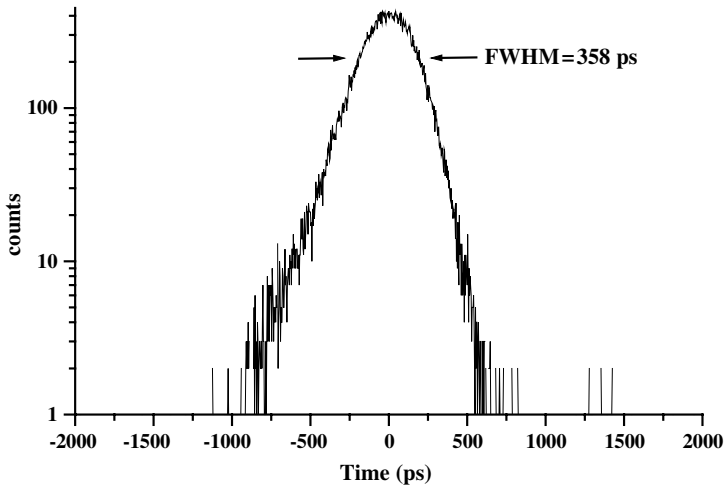

Figure 11. Coincidence timing spectrum obtained with two six-sided polished LPS:0.5% Ce crystals ($4 \times 1 \times 20$ mm^3) coupled to XP2020Q PMTs. The measurements were performed for a ^{60}Co source with an energy threshold set at $E \geqslant 1$ MeV.

(FWHM) is given by:

$$R = 2.35\sqrt{\frac{1 + \upsilon(M)}{N_{phe}}} \tag{4}$$

where $\upsilon(M)$ is the variance in the photomultiplier gain, usually about 0.1, and N_{phe} is the number of photoelectrons detected by the PMT. For LPS: Ce crystals, this fundamental limit is around 4% at 662 keV. The experimental values for the energy resolution are in the range 9–12% (table 2). Additional contributions are mentioned in the literature, such as non-proportionality in the response of the material, inhomogeneities in the crystal, non-uniformity in the light collection efficiency and non-uniformity in the photocathode performance [22, 24]. For LPS:Ce, the strong non-proportionality response could partially explain these relatively high experimental energy resolution values. Furthermore, the crystalline quality of LPS:Ce samples could be further improved, as some defects are still present in the crystals. These inhomogeneities could, in some way, affect the energy resolution.

4. Coincidence timing

The coincidence timing spectrum of LPS:Ce crystals is depicted in figure 11. The measured value (FWHM) is 358 ps, which corresponds to a time resolution of 253 ps. By comparison, LSO [25, 26] and LuAP [27] crystals have better time resolutions than LPS (about 160 ps), whereas those of GSO [28] and BGO [29] are worse (700 and 1000 ps respectively). As the time resolution value depends on the crystal size and shape [26], the relatively high value obtained for the LPS:Ce crystal could be explained by a non-optimized crystal shape.

5. Conclusion

In the search for new heavy scintillators, we have characterized the lutetium pyrosilicate material doped with the Ce^{3+} ion ($Lu_2Si_2O_7:Ce^{3+}$ or LPS:Ce), of which large sized crystals

were obtained from the melt by the Czochralski process. The outstanding features of the LPS:Ce crystals are a short decay time of 38 ns, without long components or afterglow, a high LY (about 26 300 ph MeV^{-1}) and an easy crystal growth with a moderately high melting point (1900 °C), by comparison with other materials. This makes this material an attractive new scintillator for detection of hard gamma rays and it could be used in PET or in borehole logging applications. Better energy resolution is expected by improving the crystalline quality.

Acknowledgments

This research was supported by Saint Gobain Crystals and Detectors, by French–Dutch Van Gogh exchanges and by the French Office of Industry (convention No 014906108).

References

[1] van Eijk C W E 2001 *Nucl. Instrum. Methods* A **460** 1
[2] Takagi K and Fukazawa T 1983 *Appl. Phys. Lett.* **42** 43
[3] Melcher C L and Schweitzer J S 1992 *Nucl. Instrum. Methods* A **314** 212
[4] Moses W W, Derenzo S E, Fyodorov A, Korzhik M, Gektin A, Minkov B and Aslanov V 1995 *IEEE Trans. Nucl. Sci.* **42** 275
[5] Lempicki A, Randles M H, Wisniewski D, Balcerzyk M, Brecher C and Wojtowicz A J 1995 *IEEE Trans. Nucl. Sci.* **42** 280
[6] Cooke D W, McClellan K J, Bennett B L, Roper J M, Whittaker M T and Muenchausen R E 2000 *J. Appl. Phys.* **88** 7360
[7] Kimble T, Chou M and Chai B H T 2002 *Proc. IEEE Nuclear Science Symp. Conf.* at press
[8] Pauwels D, Lemasson N, Viana B, Kahn-Harari A, van Loef E V D, Dorenbos P and van Eijk C W E 2000 *IEEE Trans. Nucl. Sci.* **47** 1787
[9] Pauwels D, Viana B, Kahn-Harari A, Dorenbos P and van Eijk C W E 2002 *US Patent Specification* 6437336
[10] Moses W W 1993 *Nucl. Instrum. Methods* A **336** 253
[11] Dorenbos P, de Haas J T M, Visser R, van Eijk C W E and Hollander R W 1993 *IEEE Trans. Nucl. Sci.* **40** 424
[12] Bretheau-Raynal F, Lance M and Charpin P 1981 *J. Appl. Crystallogr.* **14** 349
[13] Dorenbos P 2000 *J. Lumin.* **91** 155
[14] Lyu L J and Hamilton D S 1991 *J. Lumin.* **48/49** 251
[15] Dorenbos P, van Eijk C W E, Bos A J J and Melcher C L 1994 *J. Phys.: Condens. Matter* **6** 4167
[16] Dorenbos P, van Eijk C W E, Bos A J J and Melcher C L 1994 *J. Lumin.* **60/61** 979
[17] Rogers J G and Batty C J 2000 *IEEE Trans. Nucl. Sci.* **47** 438
[18] Cooke D W, Bennett B L, McClellan K J, Roper J M and Whittaker M T 2001 *J. Lumin.* **92** 83
[19] Rodnyi P A, Dorenbos P and van Eijk C W E 1995 *Phys. Status Solidi* b **187** 15
[20] van't Spijker J C 1999 *Thesis* University of Technology Delft
[21] Dorenbos P, de Haas J T M, van Eijk C W E, Melcher C L and Schweitzer J S 1994 *IEEE Trans. Nucl. Sci.* **41** 735
[22] Dorenbos P, de Haas J T M and van Eijk C W E 1995 *IEEE Trans. Nucl. Sci.* **42** 2190
[23] Balcerzyk M, Moszynski M, Kapusta M, Wolski D, Pawelke J and Melcher C L 2000 *IEEE Trans. Nucl. Sci.* **47** 1319
[24] Dorenbos P 2002 *Nucl. Instrum. Methods* A **486** 208
[25] Ludziejewski T, Moszynska K, Moszynski M, Wolski D, Klamra W, Norlin L O, Devitsin E and Kozlov V 1995 *IEEE Trans. Nucl. Sci.* **42** 328
[26] Moses W W and Derenzo S E 1999 *IEEE Trans. Nucl. Sci.* **46** 474
[27] Moszynski M, Wolski D, Ludziejewski T, Kapusta M, Lempicki A, Brecher C, Wisniewski D and Wojtowicz A J 1997 *Nucl. Instrum. Methods* A **385** 123
[28] Moszynski M, Ludziejewski T, Wolski D, Klamra W and Avdejchikov V V 1996 *Nucl. Instrum. Methods* A **372** 51
[29] Moszynski M, Gresset C, Vacher J and Odru R 1981 *Nucl. Instrum. Methods* **188** 403